



Published in final edited form as:

*Am J Ophthalmol.* 2019 July ; 203: 103–115. doi:10.1016/j.ajo.2019.01.012.

## Earliest Evidence of Preclinical Diabetic Retinopathy Revealed using Optical Coherence Tomography Angiography (OCTA) Perfused Capillary Density

Richard B. Rosen<sup>1,2,\*</sup>, Jorge S. Andrade Romo<sup>2</sup>, Brian D. Krawitz<sup>1,2</sup>, Shelley Mo<sup>1,2</sup>, Amani A. Fawzi<sup>3</sup>, Rachel E. Linderman<sup>4</sup>, Joseph Carroll<sup>4,5</sup>, Alexander Pinhas<sup>2,6</sup>, and Toco Y.P. Chui<sup>1,2</sup>

<sup>1</sup>Icahn School of Medicine at Mount Sinai, New York, NY, USA

<sup>2</sup>Ophthalmology, New York Eye and Ear Infirmary of Mount Sinai, New York, NY, USA

<sup>3</sup>Ophthalmology, Feinberg School of Medicine, Northwestern University, Chicago, IL, USA

<sup>4</sup>Cell Biology, Neurobiology & Anatomy, Medical College of Wisconsin, Milwaukee, WI, USA

<sup>5</sup>Ophthalmology & Visual Sciences, Medical College of Wisconsin, Milwaukee, WI, USA

<sup>6</sup>Ophthalmology, State University of New York Downstate Medical Center, New York, NY, USA

### Abstract

**Purpose:** To compare perfused capillary density (PCD) in diabetic patients and healthy controls using optical coherence tomography angiography (OCTA).

**Methods:** Forty controls, 36 diabetics without clinical retinopathy (NoDR), 38 with nonproliferative retinopathy (NPDR), and 38 with proliferative retinopathy (PDR) were imaged using SD-OCT. A 3×3 mm full-thickness parafoveal OCTA scan was obtained from each participant. Following manual delineation of the foveal avascular zone (FAZ), FAZ area, perimeter, and acircularity index were determined. Seven consecutive equidistant 200- $\mu$ m-wide annular segments were drawn at increasing eccentricities from the FAZ margin. Annular PCD (%) was defined as perfused capillary area divided by the corresponding annulus area after subtraction of noncapillary blood vessel areas. Nonparametric Kruskal-Wallis testing with Bonferroni correction was performed in pairwise comparisons of group PCD values.

**Results:** The NoDR group demonstrated consistently higher PCD compared to the control group in all seven annuli, reaching statistical significance ( $36.6\pm 3.30\%$  vs  $33.6\pm 3.98\%$ ,  $P=0.034$ ) at the innermost annulus (FAZ margin to 200- $\mu$ m out). The NPDR and PDR groups demonstrated progressively decreasing PCD. Differences in FAZ metrics between the NoDR and control groups did not reach statistical significance.

**Conclusions:** Relative to healthy controls, increased PCD values in the NoDR group likely represent an autoregulatory response to increased metabolic demand, while the decrease in PCD

\*Corresponding author Richard B Rosen, 310 East 14th Street, 5th Floor, South Building, New York, NY, 10003, rosen@nyee.edu.  
*Contributions of authors:* Design of the study (RBR, TYPC); Conduct of the study (RBR, JSAR, JC, TYPC); Collection and management of the data (RBR, JSAR, BDK, SM, RL, JC, TYPC); Analysis and interpretation of the data (RBR, AP, TYPC); Preparation and review of the manuscript (RBR, AAF, JC, AP, TYPC).

that follows in NPDR and PDR results largely from an incremental loss of capillary segments. These findings, consistent with previous studies, demonstrate the potential of OCTA as a clinical tool for earlier objective detection of preclinical diabetic retinopathy.

---

## INTRODUCTION

The global prevalence of diabetes mellitus has reached epidemic proportions, estimated to have affected 415 million people in 2015, and is expected to affect 642 million by 2040.<sup>1</sup> Diabetic retinopathy is the most common complication of diabetic microvascular disease, and is the leading cause of vision loss in adulthood.<sup>2</sup> Additionally, diabetes is a major cause of life-threatening complications such as end-stage renal disease,<sup>3</sup> myocardial infarction, stroke and peripheral vascular disease.<sup>4,5</sup>

Many insights into the microvascular changes that occur from long-term exposure to hyperglycemia have been gained from taking advantage of the transparency of ocular structures and examining the living retina.<sup>6</sup> The visualization of retinal vascular lesions has helped scientists and clinicians better understand the natural course of the disease.<sup>7</sup> Non-proliferative diabetic retinopathy (NPDR) has been used as an umbrella term for the clinically identifiable biomarkers of diabetic microvascular disease in the retina prior to the development of more vision-threatening proliferative changes.<sup>8</sup> The earliest clinically observable signs of NPDR include microaneurysms, capillary non-perfusion and dot-and-blot intraretinal hemorrhages.<sup>9</sup>

The ability to monitor tissue response to treatment through serial examinations of the retina has been used to guide management goals of hyperglycemia with systemic medicines such as oral hypoglycemics and insulin in attempts to lower the risk of diabetic damage to the eye as well as other micro- and macro-vascular end organ complications.<sup>10,11</sup> This approach may be more sensitive than the reverse since in some patients structural changes occur despite apparent good metabolic control.<sup>12</sup> The relative success achieved with current retinal screening and treatment protocols<sup>13</sup> has encouraged further research to identify earlier preclinical biomarkers of microvascular abnormality in the diabetic retina. The hope is that these markers will allow clinicians to diagnose disease and stratify patients according to their risk for end-organ complications earlier. This is important since earlier treatment is associated with better outcomes.<sup>14</sup> These markers would potentially allow clinicians to monitor tissue response to current and emerging systemic and ocular treatment modalities in a more sensitive and individualized manner. Novel preclinical biomarkers could also shed additional light on to the pathophysiology of diabetic microvascular disease and retinopathy.

Advances in retinal imaging and image processing techniques have allowed researchers to detect earlier signs of disease preceding classic NPDR, including structural markers such as arteriolar and venular caliber changes, tortuosity progression, and foveal avascular zone (FAZ) size and shape alterations, as well as functional markers such as vasodilatory response, blood flow and oxygen saturation variances.<sup>15</sup> A significant advancement in retinal microvascular imaging, adaptive optics scanning light ophthalmoscopy (AOSLO), was the first technology to reveal the delicate structure of capillaries at a much higher resolution than conventional fluorescein angiography (FA) in a variety of modalities,

including confocal and non-confocal techniques.<sup>16–20</sup> Advancing the lateral image resolution on clinical subjects by at least one order of magnitude (from 20- $\mu$ m to 2- $\mu$ m), AOSLO brought vascular wall components, microaneurysms, and single capillary segment details into focus.<sup>16,17,21–23</sup> Its major limitation has been the time-consuming off-line processing effort required for outputting results, which may take several hours to several days. The vascular details revealed by this laboratory technique have raised awareness of the need for an imaging technology that is capable of imaging capillary beds in a clinically relevant time scale.

Optical coherence tomography angiography (OCTA), a more recent development which takes advantage of higher speed OCT and sophisticated image processing algorithms,<sup>24–26</sup> provides very comparable quantitative and qualitative retinal microvascular details to AOSLO-FA,<sup>27</sup> and does so in 3-dimensions and with an immediacy which fosters clinical relevance. The clinical impact of this new imaging modality is still unfolding, since it provides access to functional data concealed within the structural features of the image. Some of the novel biomarkers that have been proposed include detection of nonperfused capillaries,<sup>28</sup> changes in FAZ metrics,<sup>29–31</sup> changes in perifoveal intercapillary area,<sup>32</sup> and functional markers such as adjusted flow index.<sup>33</sup>

In our laboratory, we initially developed a number of qualitative tools, including perfused vessel density calculations and vessel density color maps based on skeletonized AOSLO FA perfusion maps, to study the retinal microvasculature in healthy eyes and in eyes with venous occlusive disease.<sup>34,35</sup> A version of this method was applied to OCTA through a collaboration between members of our team and the software engineers at Optovue, enabling Agemy and associates to demonstrate that it could objectively categorize levels of progressive diabetic retinopathy consistent with expert reader interpretation.<sup>36</sup> Other similar techniques of OCTA perfusion density mapping have been developed and used to suggest that perfused vessel density is decreased in diabetic eyes without retinopathy.<sup>37–42</sup> These studies employed different variations of perfused vessel density, largely relying upon the percent area occupied by perfused vessels divided by total sampled area, and included noncapillary blood vessels in their analysis.

The purpose of this study was to assess parafoveal perfused capillary density (PCD) using OCTA, with an analysis that specifically excludes noncapillary blood vessels, in patients with diabetes but no clinical evidence of retinopathy and patients with various clinical stages of diabetic retinopathy, compared to healthy controls. Our findings suggest that OCTA PCD, after excluding noncapillary blood vessels, may be a novel and an even more sensitive biomarker for detecting the earliest diabetic changes in patients with no other evidence of clinically observable retinopathy as well as objectively monitoring the clinical course of the disease.

## METHODS

### Study Population

Written consent was obtained from all participants prior to imaging. The protocol conformed to the tenets of the Declaration of Helsinki, was HIPAA compliant and was prospectively

approved by the Institutional Review Boards of the New York Eye and Ear Infirmary of Mount Sinai and the Medical College of Wisconsin. Forty controls with no history of intraocular pathology or major systemic vascular disease were recruited for this study. Seventy-eight diabetic patients with and without retinopathy were also recruited. Diabetic patients were divided into 3 groups: 36 patients with no clinically observable diabetic retinopathy (NoDR), 38 patients with NPDR, and 38 patients with proliferative diabetic retinopathy (PDR). Seventeen of the controls were recruited at the Medical College of Wisconsin, with the rest of the study participants being recruited at the New York Eye and Ear Infirmary of Mount Sinai. All diabetic patients underwent comprehensive ophthalmic examination including slit lamp examination and dilated fundoscopy. Inclusion criteria for both healthy controls and diabetic patients were as follows: normal anterior segment and clear media. Diabetic patients without clinical retinopathy were examined by a retina specialist to rule out any presence of microaneurysms, hemorrhages, or ophthalmoscopically detectable evidence of capillary nonperfusion. Diabetic patients had a BCVA of 20/80 or better. Exclusion criteria included nuclear, cortical, or posterior subcapsular cataracts grade 3 according to the Lens Opacity Classification System III<sup>43</sup>, active macular edema and past ocular surgery including cataract and refractive surgery. Only one eye from each participant was included for imaging and data analysis.

### OCTA Image Acquisition

Utilizing a commercial spectral domain OCT system (Avanti RTVue-XR; AngioVue version 2016.2.0.16 and 2016.2.0.35; Optovue, Fremont, CA), a 3×3 mm macular OCTA scan was obtained in each participant. The scans were segmented to isolate the full vascular slab between the inner limiting membrane and 70- $\mu$ m below the posterior boundary of the inner plexiform layer, including both superficial and deep capillary layers, and noncapillary blood vessels. This OCT system has an A-scan rate of 70,000 scans per second using a light source centered at 840 nm and a bandwidth of 45 nm. Each OCTA scan was composed of two volumetric raster scans (one horizontal and one vertical) with 304 A-scans per B-scan and 608 total B-scans per volumetric raster scan. OCTA images were created using the split-spectrum amplitude decorrelation angiography (SSADA) algorithm incorporated into the device.<sup>44</sup> Individual axial length measurements were obtained using an IOL Master (Carl Zeiss Meditec, Inc., Dublin, CA) to correct the retinal magnification of each OCTA image.

### OCTA Image processing

The OCTA image processing and analysis was done in Matlab (The MathWorks, Inc., Natick, MA) and was similar to our previously published studies (Figure 1).<sup>45</sup> First, each grayscale full vascular slab OCTA image (304 × 304 pixels) was resized by a factor of six (1824 × 1824 pixels) (Figure 1A). Then, the FAZ was manually delineated creating an FAZ mask using Adobe Photoshop CS6 (Adobe System Inc., San Jose, CA) (Figure 1B, **yellow area**). FAZ metrics including area, perimeter, and acircularity index were computed based on the FAZ mask as previously described.<sup>31</sup> Global thresholding was then applied to the contrast-stretched full vascular slab OCTA by replacing all pixel intensity greater than 0.7 with the value 1 (white) and the remaining pixels with the value 0 (black) (Figure 1B, **white area**). This binary image was used as a mask for the removal of the area associated with the noncapillary blood vessels on the full vascular slab OCTA. After the removal of noncapillary

blood vessels, local thresholding was performed for the segmentation of parafoveal perfused capillaries (Figure 1C). For qualitative assessment, a color-coded PCD map was created (Figure 1D). On the PCD map, noncapillary blood vessels appear in white as they were excluded from the computation.

To ensure that the same region of interest was compared across all full vascular slab OCTA images with varying FAZ sizes and shapes, distance transformation of the FAZ mask was performed to create seven consecutive equidistant annuli of increasing retinal eccentricity from the FAZ margin, each with a width of 200- $\mu\text{m}$  (Figure 1D). The innermost annulus included the area of the retina from the FAZ margin (0- $\mu\text{m}$ ) outward to 200- $\mu\text{m}$  from the FAZ margin. The outermost annulus represented retinal distance from 1200- to 1400- $\mu\text{m}$  from the FAZ margin.

For quantitative assessment, PCD and noncapillary blood vessel density (%) for each annulus were then computed as described below:

$$\text{Perfused capillary density, \%} = \frac{\text{Perfused capillary area}}{\text{Annulus area} - \text{Noncapillary blood vessel area}} \times 100\%$$

$$\text{Noncapillary blood vessel density, \%} = \frac{\text{Noncapillary blood vessel area}}{\text{Annulus area}} \times 100\%$$

### Statistical Analysis

Statistical analysis was performed using commercial statistical software (SPSS, IBM Analytics, IBM Corporation, Armonk, NY, USA). Sex differences in FAZ metrics, PCD, and noncapillary blood vessel density were assessed using Mann-Whitney U tests. Nonparametric Kruskal-Wallis tests with Bonferonni correction for pairwise comparison were used to assess age and axial length differences between study groups.

Two-way analysis of variance (ANOVA) with post hoc Bonferonni correction was used to assess the effect of study group and annulus on PCD. Nonparametric Kruskal-Wallis testing with Bonferonni correction for pairwise comparison was used to assess differences between study groups in FAZ metrics and PCD at each annulus. A parallel analysis was performed on noncapillary blood vessel density values to ensure that there was no confounding effect of noncapillary blood vessel changes on PCD results. P-values less than 0.05 were considered statistically significant. The diagnostic capability of PCD at the 200- $\mu\text{m}$  annulus to differentiate between control and NoDR eyes was assessed using the area under the receiver operating characteristic curve (AUROC), sensitivity at 95% specificity, and specificity at 95% sensitivity.

## RESULTS

One hundred and fifty two eyes of 152 participants were analyzed (75 males, 77 females). Participant demographic information is listed in Table 1. Although females showed significantly larger FAZ areas (female:  $0.38 \pm 0.15 \text{mm}^2$  vs male:  $0.32 \pm 0.12 \text{mm}^2$ ;  $P=0.003$ )

and smaller FAZ acircularity indexes (female:  $1.39 \pm 0.24$  vs male:  $1.48 \pm 0.31$ ;  $P=0.02$ ) compared to males, no sex difference was observed in FAZ perimeter. No sex difference was observed in PCD and noncapillary blood vessel density at any annulus. There were no significant differences in age or axial length between the 4 study groups.

### FAZ Metrics

Boxplots of FAZ area, perimeter, and acircularity index are shown in Figure 2 with brackets indicating statistical significance between groups. The mean and SD values of all 3 FAZ metrics for the 4 study groups are shown in Table 2. FAZ area was significantly greater in the PDR group compared to the control and NoDR groups. Similarly, FAZ perimeter and acircularity index were significantly greater in the NPDR and PDR groups compared to the control and NoDR groups. Notably, no statistically significant difference was detected between the control and the NoDR groups in any of the FAZ metrics.

### Perfused Capillary Density

PCD group mean values per annulus are shown in Figure 3. PCD was highest in the NoDR group, followed by the control, NPDR and PDR groups. Mean PCD values and 95% confidence intervals for each annulus are displayed in Table 3. Using two-way ANOVA, a significant main effect on PCD was found between the study groups ( $P=4.81 \times 10^{-118}$ ). Post hoc analyses indicated that all four study groups differed significantly ( $P<0.0001$ ). Importantly, PCD was significantly higher in the NoDR group compared to the other three study groups. As expected, two-way ANOVA showed a significant main effect of annulus on PCD values ( $P<2.14 \times 10^{-53}$ ), with post hoc analyses indicating that PCD measured at the 200- $\mu\text{m}$  annulus was significantly lower than that of the other 6 annuli ( $P<0.0001$ ). There was no significant interaction between study group and annulus ( $P=0.27$ ).

While the NoDR group showed consistently higher PCD compared to the control group at all annuli, nonparametric Kruskal-Wallis tests indicated that only the 200- $\mu\text{m}$  annulus reached statistical significance (NoDR  $36.6 \pm 3.30\%$  vs control  $33.6 \pm 3.98\%$ ,  $P=0.034$ ; Figure 4A). In discriminating between the control versus NoDR eyes, PCD measured at the 200- $\mu\text{m}$  annulus showed an AUROC of 0.713 (95% confidence interval: 0.598 – 0.827), with sensitivity at 95% specificity of 66.7% (95% confidence interval: 0 – 90%), and specificity at 95% sensitivity of 73.5% (95% confidence interval: 38.2 – 91.2%). Boxplots of PCD measured at the 200- $\mu\text{m}$ , 800- $\mu\text{m}$ , and 1400- $\mu\text{m}$  annuli are shown in Figure 4, with brackets indicating statistically significant differences between corresponding study groups.

Color-coded PCD maps of 4 representative individual eyes, one from each of the 4 study groups, are shown in Figure 5, demonstrating qualitative and quantitative comparisons. The first column indicates the contrast-stretched full vascular slab OCTA image from each group. The second column shows the overlay of capillary segmentation (in cyan) over the full vascular slab OCTA image after removal of noncapillary blood vessels. Color-coded PCD maps are shown in the last column with the 200- $\mu\text{m}$  annulus delineated with a black border for comparison.

## Noncapillary Blood Vessel Density

Noncapillary blood vessel density group mean values per annulus are shown in Figure 3. Boxplots of noncapillary blood vessel density measured at the 200- $\mu\text{m}$ , 800- $\mu\text{m}$ , and 1400- $\mu\text{m}$  annuli are shown in Figure 4, with brackets indicating statistically significant differences between corresponding study groups. Nonparametric Kruskal-Wallis tests indicated that only the 200- $\mu\text{m}$ , 600- $\mu\text{m}$ , and 800- $\mu\text{m}$  annuli showed statistically significant differences across groups. At the 200- $\mu\text{m}$  annulus, the control group showed a significantly lower noncapillary blood vessel density compared to the PDR group (Figure 4B). At the 600- $\mu\text{m}$  and 800- $\mu\text{m}$  annuli, the NoDR group showed a significantly higher noncapillary blood vessel density compared to the PDR group (Figure 4D). No significant difference was found in noncapillary blood vessel density between the control and NoDR groups across any annulus.

## DISCUSSION

In this study, we found that the NoDR group demonstrated a consistently higher PCD compared to the healthy control group in all seven annuli, with the first annulus (FAZ margin to 200- $\mu\text{m}$  from the FAZ margin) reaching statistical significance. Notably, PCD was more sensitive than FAZ metrics for detecting a difference between these two groups. In agreement with previously reported data, NPDR and PDR groups exhibited progressively decreasing PCD.<sup>36,46</sup> Additionally, we found no significant difference in noncapillary blood vessel density between the healthy controls and NoDR patients across all annuli, which implies the capillaries as the source of the difference between these two groups. This shift from PCD elevation to progressive decline suggests a meaningful inflection or “tipping point” which may have value as a preclinical biomarker of diabetic microvascular disease, signaling that normal compensatory responses have become overwhelmed just prior to the appearance of clinically visible lesions. Exceeding this threshold is important not only for vision loss, but for other systemic complications as well. Retinal capillary beds are particularly vulnerable, showing signs of diabetic microvascular disease early due to their high metabolic demands. Though less easily recognized, other endorgans are likely not far behind.

Using OCTA, a few recent studies have reported a decrease in macular perfused vessel density in type 1 and type 2 diabetics without diabetic retinopathy compared to normal controls.<sup>37–42</sup> The major difference between those studies and ours was the way we processed the OCTA to selectively isolate the capillary change. In our study, PCD was specifically defined as the percentage of capillary area divided by the corresponding annulus area once noncapillary blood vessel areas had been subtracted. The previous studies cited included noncapillary blood vessels in the density analysis. We strongly believe that this lack of selectivity reduces the sensitivity of the analysis and misses the peak in PCD prior to its progressive decline.

Structural differences between capillaries and noncapillary blood vessels suggest that their responses to hyperglycemia may differ, and therefore removing noncapillary blood vessel areas from perfused density analysis in order to increase the sensitivity of detection of changes to the capillary bed makes sense.

The increase in PCD observed in the NoDR group could be due to new capillaries as in neovascularization, recruitment of reserve nonperfused capillary segments, or dilatation of existing capillaries. By definition, the eyes in the NoDR group did not have neovascularization, but recruitment may have contributed to a very limited extent. It is likely that dilatation of existing capillaries accounts for the bulk of the increased PCD. Capillary dilatation markedly increases volumetric retinal blood flow, by the 4<sup>th</sup> power of the lumen radius according to Poiseuille's equation. This increased blood flow through the retina in patients with diabetes mellitus without diabetic retinopathy has been reported in several studies using a variety of methods.<sup>33,47,48</sup> Furthermore, increased blood flow secondary to capillary dilatation could produce the higher intravascular oxygen concentration in arterioles that has been demonstrated using dual-wavelength oximetry in type II diabetics without diabetic retinopathy.<sup>49</sup> Conversely, blood flow has been shown to decrease in NPDR, which may be due to increased resistance from progression of capillary nonperfusion.<sup>50,51</sup>

Our methodology of determining PCD implies that our PCD results rely on a balance between capillary dilatation and capillary nonperfusion. Development of capillary segment nonperfusion in diabetic eyes must occur for some period of time before clinical retinopathy is evident.<sup>31</sup> It is likely to begin among beds of dilated capillaries resulting in some masking of a PCD reduction in the early stages. As disease worsens, nonperfusion overrides the effect on PCD of the earlier compensatory dilatation, and thus PCD first increases and then decreases. Interestingly, although previous studies showed a decreased perfused vessel density in diabetic eyes without retinopathy, they also showed an increased vessel diameter index, which is a measure for vessel caliber.<sup>37,41</sup> Furthermore, as disease worsens, blood viscosity increases and the elasticity of the vessel wall decreases, both of which would theoretically lead to decreased blood flow through the retina, leading to decreased PCD.<sup>52</sup>

Relative tissue hypoxia is thought to be an early inciting event in the pathogenesis of diabetic microvascular disease. Direct evidence of inner retinal hypoxia in diabetic cats without retinopathy has been demonstrated using an intraretinal electrode.<sup>53</sup> Several mechanisms have been proposed to account for the relative retinal hypoxia. The tissue demand for oxygen is increased, thought to be largely due to the need to accommodate increased levels of glucose. Relative hypoxia can also occur as a result of reduced oxygen extraction from blood vessels by the retinal tissues. This has been evidenced by increased venous oxygen saturation in both type 1 and 2 diabetics without diabetic retinopathy.<sup>49,54</sup> Decreased tissue oxygen extraction in diabetics may occur by shunting in the setting of subclinical capillary nonperfusion and thickening of capillary basement membranes. Ditzel<sup>55</sup> as well as Standl and Kolb<sup>56</sup> proposed that decreased oxygen extraction may be secondary to an increased oxygen affinity of hemoglobin in diabetics. Ditzel showed that at physiological blood oxygen levels, hemoglobin can release up to 30% less oxygen in diabetics.<sup>55</sup> In the setting of relative tissue hypoxia, Kohner in 1975<sup>57</sup> and Yoshida and associates in 1983<sup>58</sup> proposed that a functional capillary dilatation precedes structural changes. Many years of research later, we now know that the retinal neurovascular unit responds to tissue hypoxia (decreased pO<sub>2</sub>) and decreased pH (from increased lactic acid levels produced by anaerobic metabolism) with a functional autoregulatory dilatation of the capillaries.<sup>59</sup> In fact, several studies have shown that hyperglycemia is associated with vascular dilatation and retinal hyperperfusion.<sup>60,61</sup> Reactive oxygen species and the



inflammatory milieu in diabetes<sup>62,63</sup> likely contribute to functional capillary dilatation, as well, besides causing increased permeability, leukocyte stasis and adhesion.

Lorenzi and associates proposed another potential mechanism for increased retinal blood flow in well-controlled type 1 diabetics without retinopathy.<sup>64</sup> They reported on the absence of retinal arterial constriction in response to a pressure stimulus (reclining), attributing it to a defect in the myogenic response of the smooth muscle cells of retinal arterioles in the setting of diabetes. According to their report, this was the first detectable abnormality of the retinal vessels in these subjects. Theoretically, impaired contractility of the arterioles would cause engorgement of downstream capillary beds, manifesting as an increased PCD on OCTA imaging.

A more permanent structural dilatation may occur with prolonged functional dilatation and endothelial cell proliferation in the setting of continued hypoxia.<sup>65</sup> Increased blood flow through the dilated retinal capillaries would lead to damage to the endothelial cells; and, with concomitant pericyte loss and formation of advanced glycation end-products, would result in compromise of the microvascular wall integrity. This in turn would lead to the recognizable signs of clinical NPDR such as capillary nonperfusion, microaneurysms, and dot-and-blot hemorrhages. Fu and associates have attempted to develop a model of this proposed sequence, to explain how expanding capillary segment nonperfusion due to progressive hypoxia could lead to the larger areas of nonperfusion which follow in NPDR and PDR.<sup>66</sup>

PCD increases were highest in the innermost 200- $\mu$ m annulus surrounding the FAZ, which is consistent with the proposed model of early pathogenesis of diabetic microvascular disease. The impact of relative tissue hypoxia would be expected to be most evident adjacent to the central fovea, the region of highest metabolic demand in the retina.

Limitations of this study most notably include sample size and the demographics of the study population. Patients were self-reported diabetics. Onset of diabetes, management history, as well as blood pressure, cardiovascular health, and laboratory data such as hemoglobin A1c, blood sugar levels, and lipids were not addressed or controlled for. The permutations of these variables may also have contributed to difference in our finding compared to reports that only detected decline in PCD in their NoDR patients. A more comprehensive evaluation of these elements is planned for a future study to elucidate the impact of these factors. The contribution of insulin therapy in some of the patients in this study may have been an additional confounder. Insulin has a direct vasodilator effect on retinal arterioles via the same pathways used by capillary autoregulation – nitric oxide release in vascular endothelial cells.<sup>67</sup> While its impact on the capillary endothelium in early diabetic disease is complex, it has been shown that during later stages of diabetic retinopathy, endothelial cell insulin resistance contributes to capillary constriction and occlusion.<sup>68</sup>

The methodology of annular PCD computation is another potential source of error since it relies on manual demarcation of the FAZ margin on the OCTA image. In this study we found that FAZ does not change significantly between the control and NoDR groups, and

thus allowed for a fair comparison of annular PCD between these two groups. However, as the incidence of capillary nonperfusion surrounding the FAZ increases with worsening NPDR and PDR,<sup>36</sup> FAZ parameters change as well. Demarcating the FAZ margin on the OCTA image in the NPDR and PDR groups introduces a potential error since it is not detecting the nonperfused occluded capillaries encircling the true structural FAZ margin. This source of error can potentially be solved by delineating the FAZ margins based on the respective en face OCT reflectance images.<sup>69</sup>

OCTA is a promising non-invasive imaging modality that has the potential to reveal the earliest signs of retinal diabetic microvascular disease. The upward inflection in PCD signals a “tipping point” prior to worsening disease and may serve as a useful biomarker. The clinical significance of such a phenomenon will depend on its utility for earlier detection of retinopathy and individual risk assessment in predicting the onset of the spectrum of ocular and systemic complications of diabetes. The cross-sectional design of this study was a necessary first step. Tracking the progression in a longitudinal study through the peak of compensatory engorgement into the progressive decline in perfusion seen in NPDR and PDR eyes is potentially like watching the proverbial “canary in the coal mine.” Its recognition provides the rationale for more aggressive management of the diabetes, which can lead to reduction and potential reversal of ocular and systemic complications at earlier stages of the disease than is currently possible. Reversibility of retinal capillary damage has already been demonstrated in response to improvement in blood glucose management, following anti-VEGF therapy, and in response to therapeutic manipulation of factors such as Tie-2,<sup>70</sup> kallikrein,<sup>71</sup> and VAP-1.<sup>72</sup> Future studies should also analyze the superficial and deep parafoveal capillary networks separately, in order to determine which is more sensitive in early detection of diabetic microvascular disease in diabetic eyes without clinical retinopathy. OCTA PCD monitoring shows promise as a non-invasive detector of early diabetic retinal dysfunction, is well suited for studies of systemic pharmacologic agents targeting capillary stabilization or reperfusion,<sup>73,74</sup> and may radically alter future management of the disease.

## ACKNOWLEDGEMENTS

*Funding/Support:* The National Eye Institute of the National Institutes of Health under award numbers R01EY027301, R01EY024969 and P30EY001931. The content is solely the responsibility of the authors and does not necessarily represent the official views of the National Institutes of Health. Additional funding for this research was provided by the New York Eye and Ear Infirmary Foundation, the Marrus Family Foundation, the Geraldine Violet Foundation, and the Jorge N. Buxton MD Microsurgical Education Foundation. The sponsors and funding organizations had no role in the design or conduct of this research.

*Financial Interest Disclosures:* Richard B. Rosen receives personal fees from Nano Retina, Inc., personal fees from Astellas Pharma, Inc., personal fees and research support from Optovue, Inc., personal fees from Boehringer-Ingelheim, personal fees from Bayer, ownership interest from Guardion Health, Opticology, and GlaucoHealth outside the submitted work. Joseph Carroll receives research support from Optovue.

## BIBLIOGRAPHY

1. Ogurtsova K, da Rocha Fernandes JD, Huang Y, et al. IDF Diabetes Atlas: Global estimates for the prevalence of diabetes for 2015 and 2040. *Diabetes Res Clin Pract* 6 2017;128:40–50. [PubMed: 28437734]

2. Bourne RR, Stevens GA, White RA, et al. Causes of vision loss worldwide, 1990–2010: a systematic analysis. *Lancet Glob Health* 12 2013;1(6):e339–349. [PubMed: 25104599]
3. Saran R, Li Y, Robinson B, et al. US Renal Data System 2014 Annual Data Report: Epidemiology of Kidney Disease in the United States. *Am J Kidney Dis* 7 2015;66(1 Suppl 1):Svii, S1–305.
4. Sarwar N, Gao P, Seshasai SR, et al. Diabetes mellitus, fasting blood glucose concentration, and risk of vascular disease: a collaborative meta-analysis of 102 prospective studies. *Lancet* 6 2010;375(9733):2215–2222. [PubMed: 20609967]
5. Maffi P, Secchi A. The Burden of Diabetes: Emerging Data. *Dev Ophthalmol* 2017;60:1–5. [PubMed: 28427059]
6. Zerbini G, Maestroni S, Turco V, Secchi A. The Eye as a Window to the Microvascular Complications of Diabetes. *Dev Ophthalmol* 2017;60:6–15. [PubMed: 28427060]
7. Klein R, Lee KE, Gangnon RE, Klein BE. The 25-year incidence of visual impairment in type 1 diabetes mellitus the wisconsin epidemiologic study of diabetic retinopathy. *Ophthalmology* 1 2010;117(1):63–70. [PubMed: 19880184]
8. Jenkins AJ, Joglekar MV, Hardikar AA, Keech AC, O’Neal DN, Januszewski AS. Biomarkers in Diabetic Retinopathy. *Rev Diabet Stud* 2015 Spring-Summer 2015;12(1–2):159–195. [PubMed: 26676667]
9. Hendrick AM, Gibson MV, Kulshreshtha A. Diabetic Retinopathy. *Prim Care* 9 2015;42(3):451–464. [PubMed: 26319349]
10. Progression of retinopathy with intensive versus conventional treatment in the Diabetes Control and Complications Trial. Diabetes Control and Complications Trial Research Group. *Ophthalmology* 4 1995;102(4):647–661. [PubMed: 7724182]
11. Intensive blood-glucose control with sulphonylureas or insulin compared with conventional treatment and risk of complications in patients with type 2 diabetes (UKPDS 33). UK Prospective Diabetes Study (UKPDS) Group. *Lancet* 9 1998;352(9131):837–853. [PubMed: 9742976]
12. Cunha-Vaz J, Ribeiro L, Lobo C. Phenotypes and biomarkers of diabetic retinopathy. *Prog Retin Eye Res* 7 2014;41:90–111. [PubMed: 24680929]
13. Klein R, Klein BE. Are individuals with diabetes seeing better?: a long-term epidemiological perspective. *Diabetes* 8 2010;59(8):1853–1860. [PubMed: 20668290]
14. Pratley RE. The early treatment of type 2 diabetes. *Am J Med* 9 2013;126(9 Suppl 1):S2–9. [PubMed: 23953075]
15. Cheung CY, Ikram MK, Klein R, Wong TY. The clinical implications of recent studies on the structure and function of the retinal microvasculature in diabetes. *Diabetologia* 5 2015;58(5):871–885. [PubMed: 25669631]
16. Chui TY, Vannasdale DA, Burns SA. The use of forward scatter to improve retinal vascular imaging with an adaptive optics scanning laser ophthalmoscope. *Biomed Opt Express* 10 1 2012;3(10):2537–2549. [PubMed: 23082294]
17. Chui TY, Gast TJ, Burns SA. Imaging of vascular wall fine structure in the human retina using adaptive optics scanning laser ophthalmoscopy. *Invest Ophthalmol Vis Sci* 10 29 2013;54(10):7115–7124. [PubMed: 24071955]
18. Felberer F, Rechenmacher M, Haindl R, Baumann B, Hitzenberger CK, Pircher M. Imaging of retinal vasculature using adaptive optics SLO/OCT. *Biomed Opt Express* 4 2015;6(4):1407–1418. [PubMed: 25909024]
19. Chui TYP, Mo S, Krawitz B, et al. Human retinal microvascular imaging using adaptive optics scanning light ophthalmoscopy. *Int J Retina Vitreous* 2016;2:11. [PubMed: 27847629]
20. Morgan JJ. The fundus photo has met its match: optical coherence tomography and adaptive optics ophthalmoscopy are here to stay. *Ophthalmic Physiol Opt* 5 2016;36(3):218–239. [PubMed: 27112222]
21. Tam J, Dhamdhere KP, Tiruveedhula P, et al. Subclinical capillary changes in non-proliferative diabetic retinopathy. *Optom Vis Sci* 5 2012;89(5):E692–703. [PubMed: 22525131]
22. Burns SA, Elsner AE, Chui TY, et al. In vivo adaptive optics microvascular imaging in diabetic patients without clinically severe diabetic retinopathy. *Biomed Opt Express* 3 1 2014;5(3):961–974. [PubMed: 24688827]

23. Chui TY, Pinhas A, Gan A, et al. Longitudinal imaging of microvascular remodelling in proliferative diabetic retinopathy using adaptive optics scanning light ophthalmoscopy. *Ophthalmic Physiol Opt* 5 2016;36(3):290–302. [PubMed: 26803289]
24. Lee J, Rosen R. Optical Coherence Tomography Angiography in Diabetes. *Curr Diab Rep* 12 2016;16(12):123. [PubMed: 27766583]
25. Tan ACS, Tan GS, Denniston AK, et al. An overview of the clinical applications of optical coherence tomography angiography. *Eye (Lond)* 9 2017.
26. Choi W, Waheed NK, Moulton EM, et al. Ultrahigh Speed Swept Source Optical Coherence Tomography Angiography of Retinal and Choriocapillaris Alterations in Diabetic Patients with and without Retinopathy. *Retina* 1 2017;37(1):11–21. [PubMed: 27557084]
27. Mo S, Krawitz B, Efstathiadis E, et al. Imaging Foveal Microvasculature: Optical Coherence Tomography Angiography Versus Adaptive Optics Scanning Light Ophthalmoscope Fluorescein Angiography. *Invest Ophthalmol Vis Sci* 7 1 2016;57(9):OCT130–140. [PubMed: 27409463]
28. de Carlo TE, Chin AT, Bonini Filho MA, et al. Detection of Microvascular Changes in Eyes of Patients with Diabetes but Not Clinical Diabetic Retinopathy Using Optical Coherence Tomography Angiography. *Retina* 11 2015;35(11):2364–2370. [PubMed: 26469537]
29. Takase N, Nozaki M, Kato A, Ozeki H, Yoshida M, Ogura Y. Enlargement of Foveal Avascular Zone in Diabetic Eyes Evaluated by En Face Optical Coherence Tomography Angiography. *Retina* 11 2015;35(11):2377–2383. [PubMed: 26457396]
30. Di G, Weihong Y, Xiao Z, et al. A morphological study of the foveal avascular zone in patients with diabetes mellitus using optical coherence tomography angiography. *Graefes Arch Clin Exp Ophthalmol* 5 2016;254(5):873–879. [PubMed: 26344729]
31. Krawitz BD, Mo S, Geyman LS, et al. Acircularity index and axis ratio of the foveal avascular zone in diabetic eyes and healthy controls measured by optical coherence tomography angiography. *Vision research* 10 2017;139:177–186. [PubMed: 28212983]
32. Schottenhamml J, Moulton EM, Ploner S, et al. An Automatic, Intercapillary Area-Based Algorithm for Quantifying Diabetes-Related Capillary Dropout Using Optical Coherence Tomography Angiography. *Retina* 12 2016;36 Suppl 1:S93–S101. [PubMed: 28005667]
33. Nesper PL, Roberts PK, Onishi AC, et al. Quantifying Microvascular Abnormalities With Increasing Severity of Diabetic Retinopathy Using Optical Coherence Tomography Angiography. *Invest Ophthalmol Vis Sci* 5 2017;58(6):BIO307–BIO315. [PubMed: 29059262]
34. Pinhas A, Razeen M, Dubow M, et al. Assessment of perfused foveal microvascular density and identification of nonperfused capillaries in healthy and vasculopathic eyes. *Invest Ophthalmol Vis Sci* 11 20 2014;55(12):8056–8066. [PubMed: 25414179]
35. Pinhas A, Dubow M, Shah N, et al. FELLOW EYE CHANGES IN PATIENTS WITH NONISCHEMIC CENTRAL RETINAL VEIN OCCLUSION: Assessment of Perfused Foveal Microvascular Density and Identification of Nonperfused Capillaries. *Retina* 10 2015;35(10):2028–2036. [PubMed: 25932560]
36. Agemy SA, Scripsema NK, Shah CM, et al. Retinal Vascular Perfusion Density Mapping Using Optical Coherence Tomography Angiography in Normals and Diabetic Retinopathy Patients. *Retina* 11 2015;35(11):2353–2363. [PubMed: 26465617]
37. Kim AY, Chu Z, Shahidzadeh A, Wang RK, Puliafito CA, Kashani AH. Quantifying Microvascular Density and Morphology in Diabetic Retinopathy Using Spectral-Domain Optical Coherence Tomography Angiography. *Invest Ophthalmol Vis Sci* 7 1 2016;57(9):OCT362–370. [PubMed: 27409494]
38. Simonett JM, Scarinci F, Picconi F, et al. Early microvascular retinal changes in optical coherence tomography angiography in patients with type 1 diabetes mellitus. *Acta Ophthalmol* 12 2017;95(8):e751–e755. [PubMed: 28211261]
39. Scarinci F, Picconi F, Giorno P, et al. Deep capillary plexus impairment in patients with type 1 diabetes mellitus with no signs of diabetic retinopathy revealed using optical coherence tomography angiography. *Acta Ophthalmol* 3 2018;96(2):e264–e265. [PubMed: 28887911]
40. Dimitrova G, Chihara E, Takahashi H, Amano H, Okazaki K. Quantitative Retinal Optical Coherence Tomography Angiography in Patients With Diabetes Without Diabetic Retinopathy. *Invest Ophthalmol Vis Sci* 1 1 2017;58(1):190–196. [PubMed: 28114579]

41. Tang FY, Ng DS, Lam A, et al. Determinants of Quantitative Optical Coherence Tomography Angiography Metrics in Patients with Diabetes. *Sci Rep* 5 31 2017;7(1):2575. [PubMed: 28566760]
42. Chen Q, Ma Q, Wu C, et al. Macular Vascular Fractal Dimension in the Deep Capillary Layer as an Early Indicator of Microvascular Loss for Retinopathy in Type 2 Diabetic Patients. *Invest Ophthalmol Vis Sci* 7 1 2017;58(9):3785–3794. [PubMed: 28744552]
43. Chylack LT Jr., Wolfe JK, Singer DM, et al. The Lens Opacities Classification System III. The Longitudinal Study of Cataract Study Group. *Archives of ophthalmology (Chicago, Ill. : 1960)* 6 1993;111(6):831–836.
44. Jia Y, Tan O, Tokayer J, et al. Split-spectrum amplitude-decorrelation angiography with optical coherence tomography. *Opt Express* 2 2012;20(4):4710–4725. [PubMed: 22418228]
45. Scipesea NK, Garcia PM, Bavier RD, et al. Optical Coherence Tomography Angiography Analysis of Perfused Peripapillary Capillaries in Primary Open-Angle Glaucoma and Normal-Tension Glaucoma. *Invest Ophthalmol Vis Sci* 7 2016;57(9):OCT611–OCT620. [PubMed: 27742922]
46. Mastropasqua R, Toto L, Mastropasqua A, et al. Foveal avascular zone area and parafoveal vessel density measurements in different stages of diabetic retinopathy by optical coherence tomography angiography. *Int J Ophthalmol* 2017;10(10):1545–1551. [PubMed: 29062774]
47. Grunwald JE, DuPont J, Riva CE. Retinal haemodynamics in patients with early diabetes mellitus. *Br J Ophthalmol* 4 1996;80(4):327–331. [PubMed: 8703884]
48. Burgansky-Eliash Z, Barak A, Barash H, et al. Increased retinal blood flow velocity in patients with early diabetes mellitus. *Retina* 1 2012;32(1):112–119. [PubMed: 21878846]
49. Hafner J, Ginner L, Karst S, et al. Regional Patterns of Retinal Oxygen Saturation and Microvascular Hemodynamic Parameters Preceding Retinopathy in Patients With Type II Diabetes. *Invest Ophthalmol Vis Sci* 10 2017;58(12):5541–5547. [PubMed: 29075765]
50. Burgansky-Eliash Z, Nelson DA, Bar-Tal OP, Lowenstein A, Grinvald A, Barak A. Reduced retinal blood flow velocity in diabetic retinopathy. *Retina* 5 2010;30(5):765–773. [PubMed: 20061994]
51. Tayyari F, Khuu LA, Flanagan JG, Singer S, Brent MH, Hudson C. Retinal Blood Flow and Retinal Blood Oxygen Saturation in Mild to Moderate Diabetic Retinopathy. *Invest Ophthalmol Vis Sci* 10 2015;56(11):6796–6800. [PubMed: 26567792]
52. Feke GT, Tagawa H, Yoshida A, et al. Retinal circulatory changes related to retinopathy progression in insulin-dependent diabetes mellitus. *Ophthalmology* 11 1985;92(11):1517–1522. [PubMed: 4080324]
53. Linsenmeier RA, Braun RD, McRipley MA, et al. Retinal hypoxia in long-term diabetic cats. *Invest Ophthalmol Vis Sci* 8 1998;39(9):1647–1657. [PubMed: 9699554]
54. Fondi K, Wozniak PA, Howorka K, et al. Retinal oxygen extraction in individuals with type 1 diabetes with no or mild diabetic retinopathy. *Diabetologia* 8 2017;60(8):1534–1540. [PubMed: 28547132]
55. Ditzel J Impaired oxygen release caused by alterations of the metabolism in the erythrocytes in diabetes. *Lancet* 4 1972;1(7753):721–723. [PubMed: 4111196]
56. Standl E, Kolb HJ. 2,3-Diphosphoglycerate fluctuations in erythrocytes reflecting pronounced blood glucose variation. In-vivo and in-vitro studies in normal, diabetic and hypoglycaemic subjects. *Diabetologia* 12 1973;9(6):461–466. [PubMed: 4359285]
57. Kohner EM. Dynamic changes in the microcirculation of diabetics as related to diabetic microangiopathy. *Acta Med Scand Suppl* 1975;578:41–47. [PubMed: 1057373]
58. Yoshida A, Feke GT, Morales-Stoppello J, Collas GD, Goger DG, McMeel JW. Retinal blood flow alterations during progression of diabetic retinopathy. *Archives of ophthalmology (Chicago, Ill. : 1960)* 2 1983;101(2):225–227.
59. Antonetti DA, Klein R, Gardner TW. Diabetic retinopathy. *N Engl J Med* 3 29 2012;366(13):1227–1239. [PubMed: 22455417]
60. Grunwald JE, Riva CE, Martin DB, Quint AR, Epstein PA. Effect of an insulin-induced decrease in blood glucose on the human diabetic retinal circulation. *Ophthalmology* 12 1987;94(12):1614–1620. [PubMed: 3323985]

61. Luksch A, Polak K, Matulla B, et al. Glucose and insulin exert additive ocular and renal vasodilator effects on healthy humans. *Diabetologia* 1 2001;44(1):95–103. [PubMed: 11206417]
62. Joussen AM, Poulaki V, Le ML, et al. A central role for inflammation in the pathogenesis of diabetic retinopathy. *FASEB J* 9 2004;18(12):1450–1452. [PubMed: 15231732]
63. Zhang W, Liu H, Rojas M, Caldwell RW, Caldwell RB. Anti-inflammatory therapy for diabetic retinopathy. *Immunotherapy* 5 2011;3(5):609–628. [PubMed: 21554091]
64. Lorenzi M, Fekke GT, Pitler L, Berisha F, Kolodjaschna J, McMeel JW. Defective myogenic response to posture change in retinal vessels of well-controlled type 1 diabetic patients with no retinopathy. *Invest Ophthalmol Vis Sci* 12 2010;51(12):6770–6775. [PubMed: 20592228]
65. Sosula L. Capillary radius and wall thickness in normal and diabetic rat retinae. *Microvasc Res* 3 1974;7(2):274–276. [PubMed: 4274673]
66. Fu X, Gens JS, Glazier JA, Burns SA, Gast TJ. Progression of Diabetic Capillary Occlusion: A Model. *PLoS Comput Biol* 06 2016;12(6):e1004932. [PubMed: 27300722]
67. Alder VA, Su EN, Yu DY, Cringle SJ, Yu PK. Diabetic retinopathy: early functional changes. *Clin Exp Pharmacol Physiol Sep-Oct 1997*;24(9–10):785–788. [PubMed: 9315390]
68. Bender SB, McGraw AP, Jaffe IZ, Sowers JR. Mineralocorticoid receptor-mediated vascular insulin resistance: an early contributor to diabetes-related vascular disease? *Diabetes* 2 2013;62(2):313–319. [PubMed: 23349535]
69. Miwa Y, Murakami T, Suzuma K, et al. Relationship between Functional and Structural Changes in Diabetic Vessels in Optical Coherence Tomography Angiography. *Sci Rep* 6 28 2016;6:29064. [PubMed: 27350562]
70. Campochiaro PA, Peters KG. Targeting Tie2 for Treatment of Diabetic Retinopathy and Diabetic Macular Edema. *Curr Diab Rep* 12 2016;16(12):126. [PubMed: 27778249]
71. Kita T, Clermont AC, Murugesan N, et al. Plasma Kallikrein-Kinin System as a VEGF-Independent Mediator of Diabetic Macular Edema. *Diabetes* 10 2015;64(10):3588–3599. [PubMed: 25979073]
72. Murata M, Noda K, Kawasaki A, et al. Soluble Vascular Adhesion Protein-1 Mediates Spermine Oxidation as Semicarbazide-Sensitive Amine Oxidase: Possible Role in Proliferative Diabetic Retinopathy. *Curr Eye Res* 9 22 2017;1–10. [PubMed: 27362387]
73. Simo R, Ballarini S, Cunha-Vaz J, et al. Non-traditional systemic treatments for diabetic retinopathy: an evidence-based review. *Curr Med Chem* 2015;22(21):2580–2589. [PubMed: 25989912]
74. Roy S, Kern TS, Song B, Stuebe C. Mechanistic Insights into Pathological Changes in the Diabetic Retina: Implications for Targeting Diabetic Retinopathy. *Am J Pathol* 1 2017;187(1):9–19. [PubMed: 27846381]

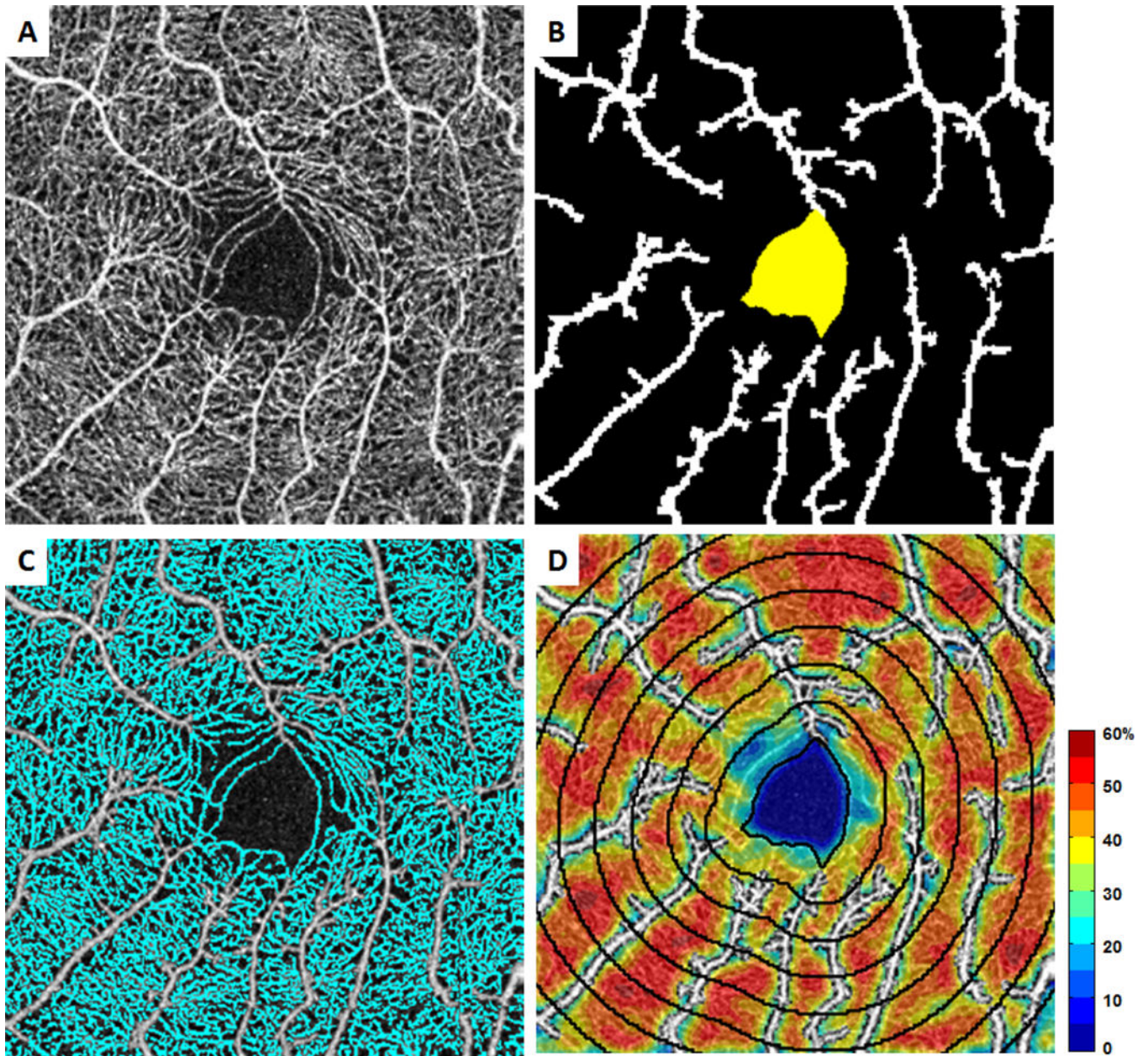


**Figure 1.** OCTA image processing procedure. A) Contrast-stretched full vascular slab OCTA. B) Manual segmentation of FAZ (in yellow) and automatic segmentation of noncapillary blood vessels using global thresholding (in white). C) Automatic segmentation of capillaries (in cyan) after the removal of noncapillary blood vessels. D) Overlay of PCD map with 7 consecutive 200- $\mu$ m equidistant annuli starting from the FAZ margin going outward.

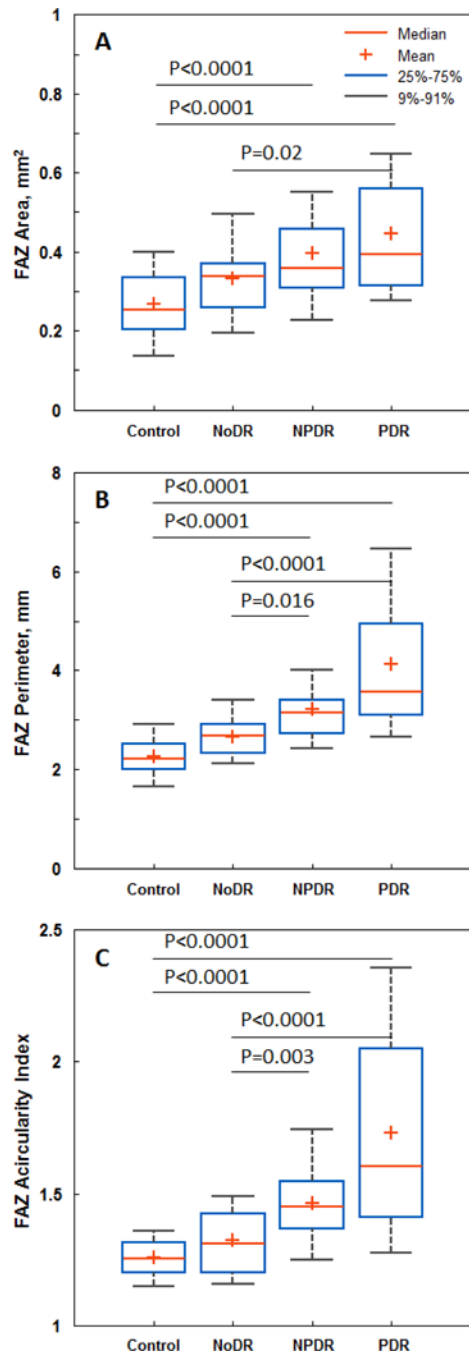


**Figure 2.** Boxplots of FAZ metrics. A) FAZ area, B) FAZ perimeter, and C) FAZ acircularity index. Brackets indicate statistical significant differences between corresponding study groups.



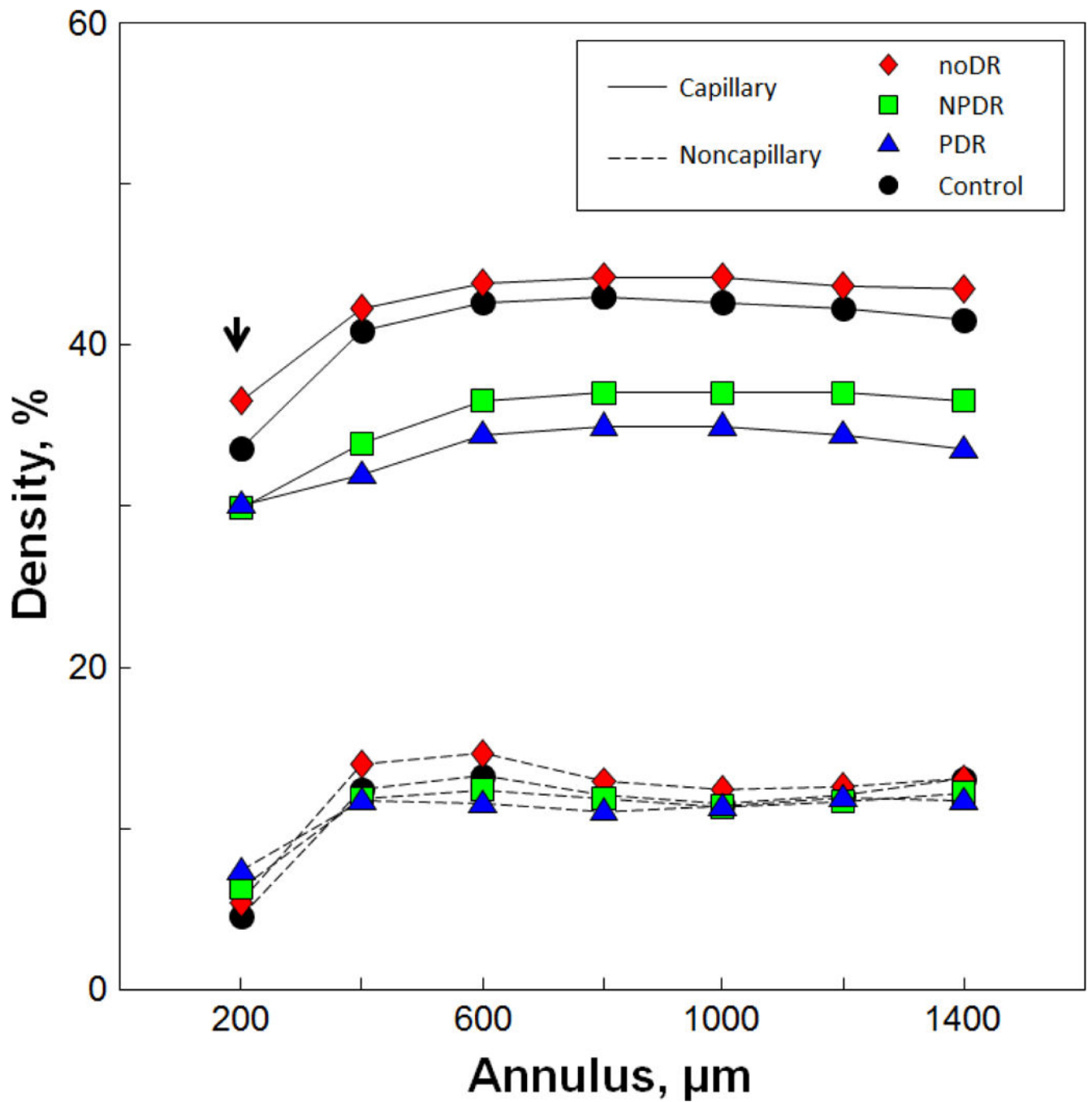


**Figure 3.** Group mean PCD and noncapillary blood vessel density values measured at each annulus. The NoDR group consistently showed higher PCD values compared to the other groups including the control group. Only the 200- $\mu\text{m}$  annulus showed a statistically significant increase in perfused capillary density in the NoDR group compared to the control group (arrow,  $P=0.034$ ).

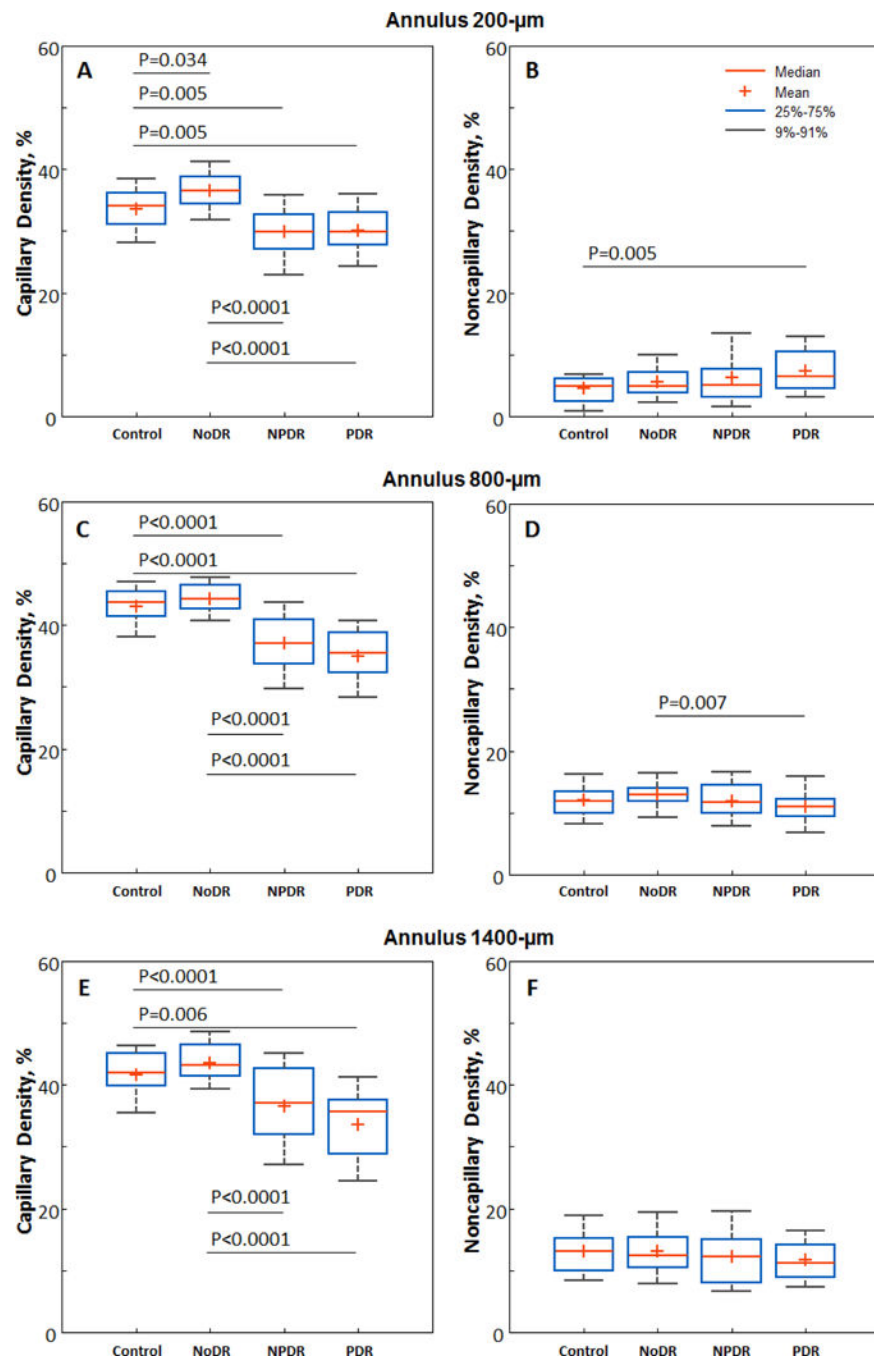


**Figure 4.** Boxplots of PCD (left column) and noncapillary blood vessel density (right column) measured at the A & B) 200- $\mu$ m, C & D) 800- $\mu$ m, and E & F) 1400- $\mu$ m annuli. Brackets indicate statistically significant differences between corresponding study groups.

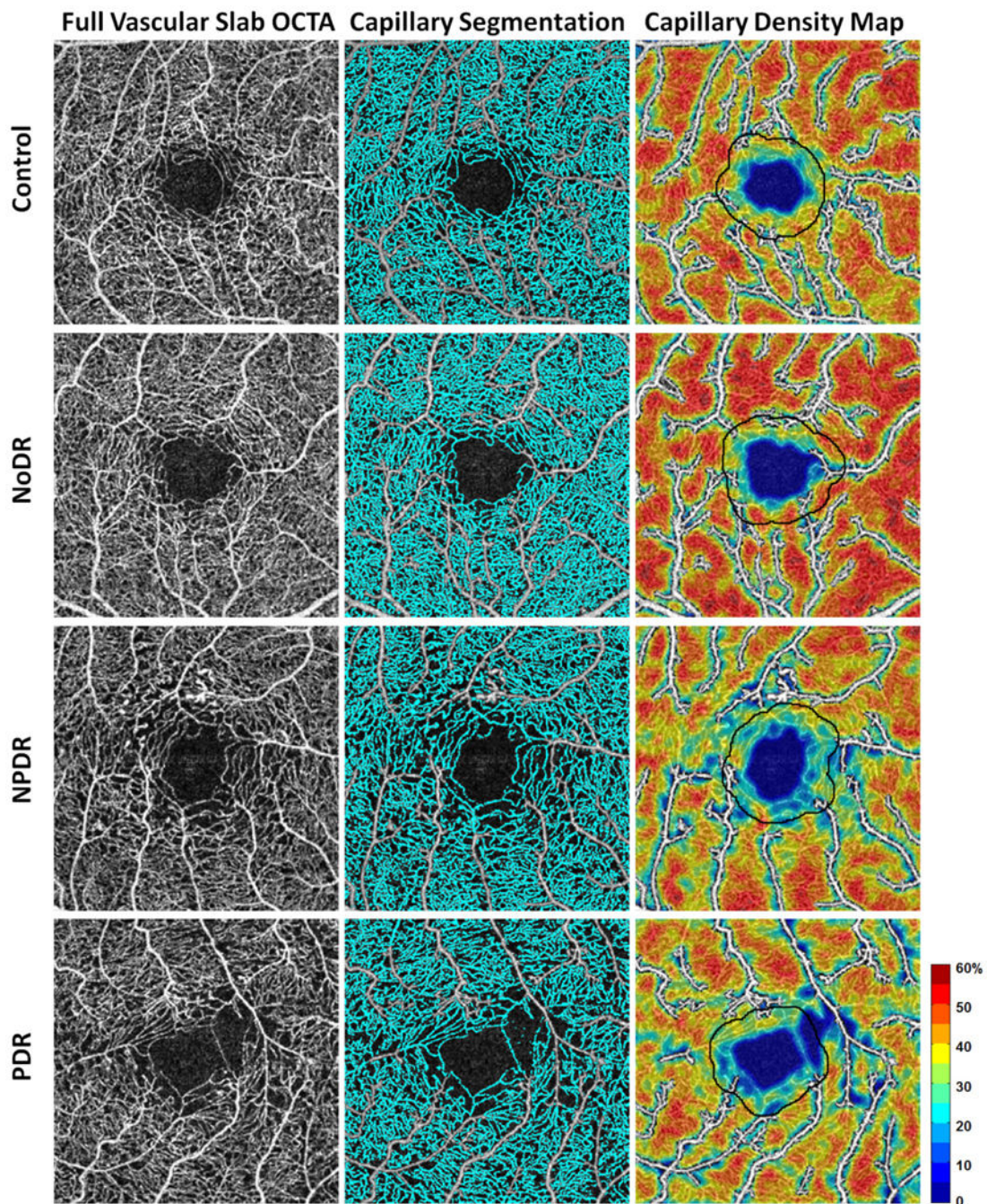


**Figure 5.** Comparison of PCD maps in a healthy control and patients with various stages of diabetic retinopathy. Left column) Contrast-stretched full vascular slab OCTA. Middle column) Corresponding capillary segmentation highlighted in cyan. Right column) Corresponding PCD maps with noncapillary blood vessels indicated in white. The 200- $\mu$ m annuli are delineated in all subjects for easier comparison.

**Table 1.**

Demographic data of the 4 study groups.

	<b>Control</b>	<b>NoDR</b>	<b>NPDR</b>	<b>PDR</b>
No. of participants	40	36	38	38
Male / Female	20/20	18/18	18/20	19/19
Mean Age $\pm$ SD, years	59.7 $\pm$ 7.89	57.69 $\pm$ 9.59	58.34 $\pm$ 6.81	55.58 $\pm$ 5.18
DM Type I / II	NA	2/34	4/34	3/36

Author Manuscript

Author Manuscript

Author Manuscript

Author Manuscript

**Table 2.**

FAZ metrics of the 4 study groups.

	<b>Control</b>	<b>NoDR</b>	<b>NPDR</b>	<b>PDR</b>
FAZ Area Mean $\pm$ SD, mm <sup>2</sup>	0.27 $\pm$ 0.09	0.33 $\pm$ 0.10	0.40 $\pm$ 0.16	0.45 $\pm$ 0.19
FAZ Perimeter Mean $\pm$ SD, mm	2.27 $\pm$ 0.44	2.66 $\pm$ 0.51	3.22 $\pm$ 0.79	4.12 $\pm$ 1.72
FAZ Acircularity Index Mean $\pm$ SD	1.26 $\pm$ 0.08	1.32 $\pm$ 0.15	1.46 $\pm$ 0.16	1.73 $\pm$ 0.42

Author Manuscript

Author Manuscript

Author Manuscript

Author Manuscript

**Table 3.**

Group mean PCD values and 95% confidence intervals measured at each annulus.

Annulus	Mean PCD % (95% Confidence Interval)			
	Control	NoDR	NPDR	PDR
200- $\mu\text{m}$	33.6 (32.4–34.9)	36.6 (35.5–37.8)	29.8 (28.2–31.4)	30.1 (28.8–31.4)
400- $\mu\text{m}$	41.0 (39.9–42.1)	42.4 (41.5–43.2)	33.9 (32.3–35.4)	32.1 (30.5–33.7)
600- $\mu\text{m}$	42.8 (41.6–43.9)	44.0 (43.2–44.9)	36.5 (34.9–38.2)	34.5 (32.8–36.2)
800- $\mu\text{m}$	43.1 (41.8–44.3)	44.3 (43.4–45.2)	37.1 (35.4–38.9)	35.0 (33.4–36.6)
1000- $\mu\text{m}$	42.7 (41.2–44.1)	44.2 (43.3–45.1)	37.1 (35.2–39.1)	35.0 (33.3–36.6)
1200- $\mu\text{m}$	42.5 (41.0–43.9)	43.8 (42.7–44.9)	37.1 (35.1–39.1)	34.5 (32.5–36.4)
1400- $\mu\text{m}$	41.6 (40.1–43.1)	43.6 (42.5–44.8)	36.7 (34.4–38.9)	33.6 (31.4–35.7)

Author Manuscript

Author Manuscript

Author Manuscript

Author Manuscript